Hippo (YAP)–autophagy axis protects against hepatic ischemia-reperfusion injury through JNK signaling

Shuguang Zhu[1], Xiaowen Wang[2], Haoqi Chen[3], Wenfeng Zhu[4], Xuejiao Li[2], Ruiwen Cui[5], Xiaomeng Yi[6], Xiaolong Chen[4], Hua Li[1], Genshu Wang[7]

[1]Department of Hepatic Surgery, Liver Transplantation, The Third Affiliated Hospital of Sun Yat-sen University, Guangzhou, Guangdong 510630, China;
[2]Department of Hepatology lab, The Third Affiliated Hospital of Sun Yat-sen University, Guangzhou, Guangdong 510630, China;
[3]Department of General Surgery, The Third Affiliated Hospital of Sun Yat-sen University, Guangzhou, Guangdong 510630, China;
[4]Department of Organ Transplantation, The Third Affiliated Hospital of Sun Yat-sen University, Guangzhou, Guangdong 510630, China;
[5]Department of Renal Transplantation, Guangdong Provincial Hospital of Chinese Medicine, Guangzhou, Guangdong 510630, China;
[6]Department of Surgical Intensive Care Unit, The Third Affiliated Hospital of Sun Yat-sen University, Guangzhou, Guangdong 510630, China;
[7]Department of Hepatic Surgery, Liver Transplantation, Guangdong Provincial Hospital of Chinese Medicine, Guangzhou, Guangdong 510630, China.

Abstract

Background: Hepatic ischemia-reperfusion injury (HIRI) remains a common complication during liver transplantation (LT) in patients. As a key downstream effector of the Hippo pathway, Yes-associated protein (YAP) has been reported to be involved in various physiological and pathological processes. However, it remains elusive whether and how YAP may control autophagy activation during ischemia-reperfusion.

Methods: Human liver tissues from patients who had undergone LT were obtained to evaluate the correlation between YAP and autophagy activation. Both an *in vitro* hepatocyte cell line and *in vivo* liver-specific *YAP* knockdown mice were used to establish the hepatic ischemia-reperfusion models to determine the role of YAP in the activation of autophagy and the mechanism of regulation.

Results: Autophagy was activated in the post-perfusion liver grafts during LT in patients, and the expression of YAP positively correlated with the autophagic level of hepatocytes. Liver-specific knockdown of *YAP* inhibited hepatocytes autophagy upon hypoxia-reoxygenation and HIRI (P <0.05). YAP deficiency aggravated HIRI by promoting the apoptosis of hepatocytes both in the *in vitro* and *in vivo* models (P <0.05). Attenuated HIRI by overexpression of YAP was diminished after the inhibition of autophagy with 3-methyladenine. In addition, inhibiting autophagy activation by *YAP* knockdown exacerbated mitochondrial damage through increasing reactive oxygen species (P <0.05). Moreover, the regulation of autophagy by YAP during HIRI was mediated by AP1 (c-Jun) N-terminal kinase (JNK) signaling through binding to the transcriptional enhanced associate domain (TEAD).

Conclusions: YAP protects against HIRI by inducing autophagy via JNK signaling that suppresses the apoptosis of hepatocytes. Targeting Hippo (YAP)–JNK–autophagy axis may provide a novel strategy for the prevention and treatment of HIRI.

Keywords: YAP-signaling proteins; Autophagy; c-Jun N-terminal kinase; Ischemia-reperfusion injury; Liver transplantation

Introduction

Hepatic ischemia-reperfusion injury (HIRI) refers to the damage that occurs after the restoration of blood flow to ischemic or hypoxic liver tissue, which consists of two independent but closely related stages: ischemic insult and reperfusion injury.[1] Currently, multiple efficient bleeding control techniques and a deeper understanding of liver physiology have promoted a rapid advancement of hepatic surgery in recent years. However, HIRI remains a common complication of hemorrhagic shock, liver trauma, partial hepatectomy, and liver transplantation (LT).[2,3] As the main increased risk contributing to liver failure and death after major hepatectomy and LT, HIRI has been reported to take up to 42.9% of early liver dysfunction.[4] Prevention serves as the main strategy to reduce HIRI

Access this article online

Quick Response Code:

Website: www.cmj.org

DOI: 10.1097/CM9.0000000000002727

Shuguang Zhu, Xiaowen Wang, Haoqi Chen, and Wenfeng Zhu contributed equally to this work.

Correspondence to: Dr. Xiaolong Chen, Department of Organ Transplantation, The Third Affiliated Hospital of Sun Yat-sen University, Guangzhou, Guangdong 510630, China
E-Mail: chxlong3@mail2.sysu.edu.cn;
Prof. Hua Li, Department of Hepatic Surgery, Liver Transplantation, The Third Affiliated Hospital of Sun Yat-sen University, Guangzhou, Guangdong 510630, China
E-Mail: lihua3@mail.sysu.edu.cn;
Prof. Genshu Wang, Department of Hepatic Surgery, Liver Transplantation, Guangdong Provincial Hospital of Chinese Medicine, Guangzhou, Guangdong 510630, China
E-Mail: wgsh168@163.com

Copyright © 2024 The Chinese Medical Association, produced by Wolters Kluwer, Inc. under the CC-BY-NC-ND license. This is an open access article distributed under the terms of the Creative Commons Attribution-Non Commercial-No Derivatives License 4.0 (CCBY-NC-ND), where it is permissible to download and share the work provided it is properly cited. The work cannot be changed in any way or used commercially without permission from the journal.

Chinese Medical Journal 2024;137(6)
Received: 16-11-2022; **Online:** 26-05-2023; **Edited by:** Jing Ni

since there is no effective therapeutic treatment. Therefore, it is of great clinical significance to explore the mechanism of HIRI and to develop new drug targets for the prevention and treatment.

Autophagy is an evolutionary conservative lysosome-dependent degradation pathway in eukaryotic cells.[5] Following the degradation of the substrates, the products are recycled back into the cytosol.[6] During starvation, growth factors deficiency, hypoxia, and reactive oxygen species (ROS) accumulation, autophagy is rapidly upregulated to degrade superfluous proteins and damaged organelles for the recycling of energy and matter, allowing cells to adapt to stress states.[7,8] Hence, autophagy has been generally considered a protective mechanism of cells, which can maintain cell survival upon stress stimulation. HIRI is mainly characterized by ischemia, hypoxia, oxidative stress, and aseptic inflammation. Recent studies have reported the protective role of autophagy in HIRI among different organs.[9,10] However, some studies stated that autophagy was termed as the type two programmed cell death, and autophagic cell death promoted cell apoptosis, especially in cardiac ischemia-reperfusion (I/R) injury.[11,12] Therefore, the role of autophagy in HIRI remains unclear, and requires further investigation.

Hippo pathway is a cascade of enzymes that phosphorylate and activate the nuclear Dbf2-related family kinase large tumor suppressor 1/2 (LATS 1/2) via the kinase mammalian sterile-20-like 1/2 (Mst 1/2), and then phosphorylate Yes-associated protein (YAP).[13] As a key effector of Hippo pathway, YAP plays a crucial role in the regulation of organ size and volume, carcinogenesis, tissue regeneration, and stemness of cells.[14,15] Several studies have shown that YAP is involved in the repairment of parenchymal organs such as the heart, brain, and kidney after I/R injury.[16,17] However, a more detailed mechanism of YAP alleviating HIRI is lacking. A recent study reported that activation of YAP attenuated HIRI by diminishing oxidative stress, necrosis/apoptosis, and suppressing the innate inflammatory response.[18] Therefore, there is an urgent need to determine the role of YAP in HIRI, and the relationship between YAP and autophagy considering the essential but inconclusive role of autophagy in HIRI.

In this study, peri- and post-reperfusion liver grafts from LT patients were collected and both *in vitro* and *in vivo* hepatic I/R models were established using hepatocyte cell and liver-specific *YAP* knockdown mice. We found that YAP played an important role in HIRI by regulating autophagy through Jun N-terminal kinase (JNK) signaling. Targeting the hippo (YAP)-JNK-autophagy axis may provide a novel prevention and treatment strategy for I/R.

Methods

Ethical approval

Ethical approval for animal experiments was obtained from the South China Agricultural University Animal Ethics Committee (approval No. RGBIO 2022012501). The experiments on mice were carried out according to the principles and guidelines of animal care and use formulated by the South China Agricultural University (Guangzhou, China). For patients, informed consent was obtained from all patients in accordance with the Ethics Committee of the Third Affiliated Hospital of Sun Yat-sen University (approval No: [2022]02-485).

Clinical liver graft samples

Peri-perfusion liver graft tissue samples from 100 orthotopic liver transplantation (OLT) patients were collected separately within 5 h of cold storage (before implantation), and post-perfusion samples were collected within 3 h after portal reperfusion (before abdominal closure). The tissues stored in liquid nitrogen were used for western blotting analysis and samples immobilized in 4% paraformaldehyde were used for histochemical analysis.

Warm hepatic I/R mouse model and treatments

Liver-specific *YAP* knockdown (*YAP*-LKD) mice were constructed first before the establishment of non-lethal models of segmental (70%) warm I/R that were described previously.[19,20] *YAP*-LKD mice were generated by crossing albumin-Cre (*Alb-Cre*) and $YAP^{flox/flox}$ mice by the Model Animal Research Center of Nanjing University (Nanjing, China). Genotyping was confirmed by polymerase chain reaction (PCR). Wild-type (WT) C57BL/6J mice (animal experiment qualification certificate No: 2018-60-14, male, 6–8 weeks old) were purchased from South China Agricultural University. Briefly, partial ischemia (70%) was performed through occlusion of the portal triad (including the portal vein, hepatic artery, and bile duct) to the left and median liver lobes for 90 min. Mice were sacrificed 6 h after reperfusion, after which liver tissue and blood samples were collected [Supplementary Figure 1, http://links.lww.com/CM9/B588]. Sham-operated controls underwent the same procedure without vascular occlusion. In some experiments, WT mice were infected with YAP adeno-associated virus (adeno-associated virus [AAV] GeneChem, Shanghai, China) through the hydrodynamic tail vein (titer: 1×10^{12} vector genome [v.g.]/mL, dose: 1.5×10^{11} v.g.), and samples were obtained three weeks after I/R models were established. And the JNK inhibitor anthrapyrazolone (SP600125; 10 mg/kg, Selleck Chemicals, Texas, USA) and the autophagy inhibitor 3-methyladenine (3-MA, 15 mg/kg, Selleck Chemicals) were intraperitoneally administered to mice 1 h before the I/R according to experimental requirements.

Cell culture

Cell hypoxia/reoxygenation (H/R) models were constructed to mimic I/R as previous studies described.[19,20] Briefly, THLE2 (ATCC, Rockefeller, USA) cells were cultured in sugar-free and serum-free dulbecco's modified eagle medium (DMEM, Gibco, Grand Island, USA) for 6 h in a humid sealed chamber with 1% O_2–5% CO_2–94% N_2 equilibrium. Cells were then incubated at 37°C for 8 h in a 95% O_2–5% CO_2 atmosphere within normal complete medium (90% DMEM and 10% fetal bovine serum, Gibco).

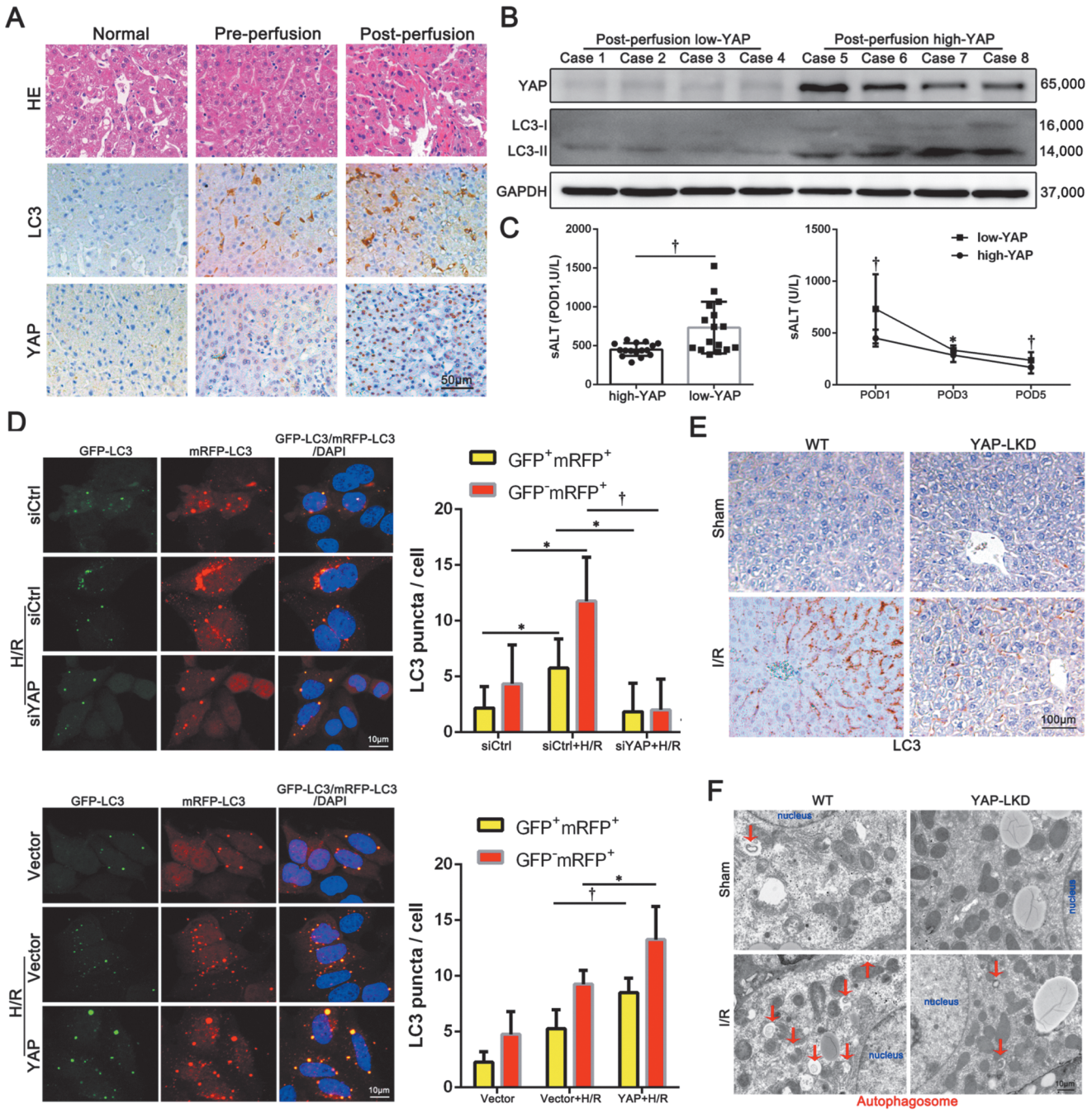

Figure 1: YAP was involved in autophagy activation during HIRI. (A) Samples of normal (n = 20), peri- and post-reperfusion liver tissues (n = 100) from patients were collected. HE staining and immunohistochemical staining for LC3 and YAP were analyzed microscopically; (B) Representative immunoblotting profiles of YAP and LC3 in liver samples were shown; (C) Serum ALT levels between groups at POD1, at each time point postoperatively were analyzed; (D) THLE2 cells subjected to H/R were transfected with GFP-mRFP-LC3 and then treated with control siRNA or YAP siRNA (left), or vector or YAP plasmid (right). Fluorescent pictures indicating autophagy activity were analyzed by confocal microscopy and LC3 puncta were determined; (E–F) Liver samples from WT mice and YAP-LKD mice in the sham group or I/R group were collected. Immunohistochemistry for LC3 was analyzed microscopically (E); Autophagosomes were detected by transmission electron microscopy (F). Red arrows represent autophagosomes; All statistical analyses were performed by Student's t-test, $^{*}P$ <0.05, and $^{\dagger}P$ <0.01 compared between groups. ALT: Alanine transaminase; GAPDH: Glyceraldehyde-3-phosphate dehydrogenase; GFP: Green fluorescent protein; HE: Hematoxylin-eosin; HIRI: Hepatic ischemia-reperfusion injury; H/R: hypoxia/reoxygenation; I/R: Ischemia/reperfusion; LC3: Light chain 3; LKD: Liver-specific knockdown; LT: Liver transplantation; mRFP: Monomeric red fluorescent protein; POD: Postoperative day; sALT: Serum alanine transaminase; siRNA: Small interfering RNA; WT: Wild-type; YAP: Yes-associated protein.

For drug administrations, THLE2 cells were treated with 3-MA (5 mmol/L, Selleck Chemicals) for 6 h or JNK inhibitor SP600125 (20 μmol/L, Selleck Chemicals) for 24 h or Verteporfin (VP, 1 μmol/L, Millipore Sigma, Bedford, MA) for 24 h. Small interfering RNA (siRNA) and plasmids were used to modulate the expression of YAP. YAP-siRNA (RiboBio, Guangzhou, China), YAP-overexpressing plasmid (GeneCopoeia, Maryland, USA), YAP-5SA plasmid (GeneCopoeia), and YAP-5SA-S94A plasmid (GeneCopoeia) were transfected using Lipofectamine 3000 (Invitrogen, California, USA) according to the manufacturer's instructions. All transfections were independently performed at

least three times. Additionally, the green fluorescent protein (GFP)-monomeric red fluorescent protein (mRFP)-LC3 lentivirus was used to measure the autophagic activity of THLE2 cells during H/R. The GFP-mRFP-LC3 lentivirus was purchased from GeneChem (Shanghai, China).

Western blotting

Western blotting analysis of whole cell lysates from cells and liver tissue were performed according to the manufacturer's instructions (Beyotime, Shanghai, China). Equal concentrations of protein from cells and liver tissue were separated by 12.5% sodium dodecyl sulfate-polyacrylamide (SDS-PAGE) gel electrophoresis and transferred to polyvinylidene fluoride (PVDF) membranes (Millipore, Bedford, MA). Subsequently, the membranes were incubated overnight at 4°C with specific antibodies against the following proteins: YAP, phospho-YAP (p-YAP), light chain 3 type B (LC3B), autophagy-related gene 5 (Atg5), caspase-3, cleaved-caspase-3, B-cell lymphoma-2 (BCL-2), BCL2-associated X (Bax), sequestosome-1 (p62), phospho Akt (Thr308), phospho-Akt (p-Akt), extracellular regulated protein kinases (Erk), phospho-Erk (p-Erk), JNK, phospho-JNK (p-JNK), p38, phospho-p38 (p-p38), Histone-3, β-actin, and glyceraldehyde-3-phosphate dehydrogenase (GAPDH) (1:1000 dilution, Cell Signaling Technology, MA, USA). The next day, membranes were incubated with a horseradish peroxidase-conjugated anti-rabbit or mouse antibody at room temperature. The signal detection and result record were finished by Tanon-5200CE Chemiluminescent Imaging System (Tanon Science and Technology, Shanghai, China).

RNA isolation and quantitative real-time reverse transcription-PCR

Total RNA was extracted using Trizol (Roche, Basel, Switzerland). Reverse transcription of total RNA (1.5 μg) with a Revert Aid First Strand complementary DNA (cDNA) synthesis kit (Roche) according to the manufacturer's instructions. Quantitative polymerase chain reaction assay (qPCR) was performed using the Synergy Brands (SYBR) green I master kit (Roche) on LightCycler 480 (Roche). Data were analyzed using the $2^{-\Delta\Delta Ct}$ method, and β-actin RNA was used as endogenous control. Primers for YAP are as follows: forward: 5′-TGAGATCCCTGATGATGTACCAC-3′, and reverse: 5′-TGTTGTTGTCTGATCGTTGTGAT-3′. Primers for β-actin are as follows: forward: 5′-CATGTACGTTGC TATCCAGGC-3′, and reverse: 5′-CTCCTTAATGTCAC GCACGAT-3′ , which was used as a reference for normalization.

Hematoxylin-eosin (HE) staining and immunohistochemical (IHC) staining

Liver tissues were fixed in 4% paraformaldehyde, embedded in paraffin and then cut into sections in 4 mm thickness. Liver tissues sections were stained with hematoxylin and eosin for histological examination using standard histological procedures. The liver sections were blindly analyzed for liver tissue injury using modified Suzuki's[21] criteria. The necrotic area and Suzuki score of all the liver sections were independently assessed by two pathologists. For immunohistochemical staining, after dewaxed, hydrated, antigen repaired, the sections were incubated with corresponding primary antibodies overnight at 4°C, including YAP, LC3B and p-JNK (1:200 dilution, Cell Signaling Technology). After washed twice with phosphate buffer saline (PBS), the sections incubated with horseradish peroxidase (HRP)-linked secondary antibody (DAKO, Glostrup, Denmark) for 1 h at room temperature. At last, the sections were visualized using diazaborine (DAB)(DAKO) and counterstained using hematoxylin.

Co-immunoprecipitation

Proteins were extracted from cells using the NETN buffer (50 mmol/L Tris 7.5, 1 mmol/L ethylene diamine tetraacetie acid (EDTA), 0.5% nonidet P-40 lysis buffer (NP-40), 5% glycerol, 150 mmol/L sodium chloride), cOmplete™ EDTA-free protease inhibitor cocktail (Sigma), and PhosSTOP™ phosphatase inhibitor cocktail (Sigma) for 30 min at 4°C. Insolvable debris was removed by centrifugation. Following preclearing, magnetic protein A/G beads were added to precipitate protein–antibody complex overnight at 4°C. After four washes in NETN buffer, immunoprecipitated proteins were eluted with laemmli protein sample buffer. Finally, immunoprecipitated complexes were subjected to 12.5% SDS-PAGE gel electrophoresis for immunoblotting analysis.

Immunofluorescence triple-labeling of YAP, p-JNK, and LC3B

Immunofluorescence multiple-labeled staining was carried out using a tyramide signal amplification (TSA)-Kit (PerkinElmer Life Sciences, Massachusetts, USA). Firstly, the sections were incubated with the primary antibody p-JNK overnight at 4℃. Then, the sections were incubated with the HRP-labeled secondary antibody for 50 min after cleaning. At last, the sections were incubated with fluorescein isothiocyanate isomer I (FITC)-TSA for 10 min after cleaning. Antigen retrieval was performed by heating in a microwave. The sections were then incubated with the primary antibody YAP overnight at 4℃ followed by incubation of the HRP-labeled secondary antibody for 50 min after cleaning. After that, the sections were incubated with 647-TSA for 10 min after cleaning. Antigen retrieval was again performed by heating in a microwave. Next, the sections were incubated with the primary antibody LC3B overnight at 4℃. Then, the sections were again incubated with the Cyanine3 (Cy3)-labeled fluorescent secondary antibody for 50 min after cleaning. Finally, the sections were incubated with 4, 6-diamino-2-phenyl indole (DAPI, 1:500 dilution; Vector Laboratories, CA, USA), and observed under fluorescence microscope.

Cell apoptosis and mitochondrial stability detection

A frozen section ROS assay kit (BestBio, Shanghai, China) was used to detect ROS levels in the tissues. A terminal deoxynucleotidyl transferase-mediated dUTP-

digoxigenin nick end labeling (Tunel) assay kit was used (Beyotime) to detect apoptotic cells in liver tissues, according to the manufacturer's instructions. Finally, the sections were incubated with DAPI (1:500 dilution; Vector Laboratories) and observed under a fluorescence microscope; The MitoSox™ Red mitochondrial superoxide indicator (Invitrogen) was used for mitochondrial ROS detection. An annexin V-FITC apoptosis detection kit (Beyotime) was used to detect apoptotic cells. The cells were analyzed using a CytoFLEX cytometer (Beckman Coulter, California, USA).

Transmission electron microscopy (TEM) analysis

TEM was used for the detection of autophagosomes. Liver tissues were fixed with 2.5% glutaraldehyde at pH 7.4, 0.1 mol/L sodium cacodylate for 2–4 h at 44°C, post-fixed, dehydrated, embedded, cut, and stained. Finally, the images were captured using an HT7700 TEM (HITACHI, Tokyo, Japan). Ultrastructural assessment was performed by a blinded analyst, and at least three randomly selected areas were evaluated.

Statistical analysis

Qualitative data are representative of at least three independent experiments. Quantitative data are presented as mean ± standard error of mean. Statistical differences between multiple groups were compared using a one-way analysis of variance. Statistical differences between the two groups were determined using a two-tailed unpaired Student's *t*-test. $P < 0.05$ was considered statistically significant. All analyses were performed using SPSS software (version 25.0, IBM, Chicago, IL, USA).

Results

YAP was involved in autophagy activation during HIRI

To evaluate the autophagy levels, YAP activation and their relationship during HIRI, peri- and post-perfusion liver grafts from LT patients ($n = 100$) and normal liver tissues from hemangioma margin ($n = 20$) were collected. The ischemia-reperfusion injury (IRI) was assessed by HE staining. As indicated by the pathology results shown in Figure 1A, post-perfusion livers showed typical IRI characteristics with parenchymal cell damage and inflammatory cell infiltration, which were not observed in normal and peri-perfusion liver tissues. The expression of autophagy-specific proteins LC3 was at baseline in normal livers, slightly upregulated in peri-perfusion grafts, but elevated in post-perfusion liver sections, indicating that autophagy was activated during IRI. Moreover, the change of YAP expression showed a similar trend as autophagy levels during the OLT [Figure 1A; Supplementary Figure 2A, C, http://links.lww.com/CM9/B588]. To further assess the relationship between YAP expression and autophagy levels, liver graft samples were divided into the high-YAP expression group and the low-YAP group by western blotting analysis ($n = 32$) [Figure 1B; Supplementary Figure 2B, http://links.lww.com/CM9/B588]. A positive correlation between autophagy (determined by LC3-II/LC3-I ratio) and YAP expression level was found [Supplementary Figure 2D, http://links.lww.com/CM9/B588]. In addition, postoperative liver enzymes (alanine transaminase, ALT) of the post-perfusion high-YAP group were significantly lower than that of the low-YAP group, and YAP expression was negatively correlated with the level of liver enzymes after OLT [$P < 0.05$, Figure 1C; Supplementary Figure 2E, http://links.lww.com/CM9/B588].

To determine the role of YAP in autophagy during I/R, an *in vitro* model of H/R to simulate I/R was established with THLE2 cells at first. Compared to the control group, autophagy was sufficiently activated during H/R stress as indicated by the significant increase of GFP-LC3 and mRFP-LC3 puncta. And overexpression of YAP further elevated the autophagy levels of cells subjected to H/R stress. In contrast, endogenous knockdown of YAP remarkably diminished the elevation of H/R stress-induced autophagy activation [$P < 0.05$, Figure 1D]. In addition, the elevation of autophagy-related proteins LC3-II and Atg5 induced by H/R stress were also diminished in the YAP deficiency group shown by western blotting analysis, while the expression of p62 that indicates autophagy flux was increased [Supplementary Figure 2F, http://links.lww.com/CM9/B588]. Besides, a mouse I/R model was established to explore the effect of YAP regulation on autophagy. Given the important role of YAP in cell biology, *YAP* knockout mice cannot survive. *YAP*-LKD mice and WT littermates were subjected to 90 min of warm ischemia followed by 6 h of reperfusion and then liver specimens were collected. Consistent with the *in vitro* results, the increased autophagy levels induced by I/R injury was attenuated in YAP-LKD mice [Figure 1E; Supplementary Figure 2G, http://links.lww.com/CM9/B588]. The TEM analysis results also revealed that the knockdown of *YAP* decreased the number of intracellular autophagosomes in mice subjected to HIRI [Figure 1F].

Protective effect of YAP on HIRI depended on activating autophagy

We further explored the role of YAP in HIRI and whether YAP exerted its function by regulating autophagy. Compared with the WT group, YAP-LKD mice showed notably exacerbated I/R-induced liver injury by histological assays, and this finding was further demonstrated by the significantly increased Suzuki score and necrosis area [$P < 0.05$, Figure 2A], as well as the elevation of liver injury parameters (serum ALT and aspartate transaminase [AST]) and inflammatory cytokines (serum interleukin 6 [IL-6] and tumor necrosis factor-α [TNF-α]) [$P < 0.05$, Figure 2B, C]. These results suggested that YAP played a protective role in HIRI. Thus, we then explored whether YAP protected hepatocytes against IR injury by modulating autophagy. WT mice subjected to HIRI were treated with the autophagy inhibitor 3-MA after AAV-YAP transfection. YAP was found to play a protective role during I/R, as evidenced by the lower Suzuki score, smaller necrotic area, reduced liver enzymes, and attenuated inflammatory cytokines observed in AAV-YAP mice compared to the AAV-vector group [$P < 0.05$, Figure 2D–F]. After the

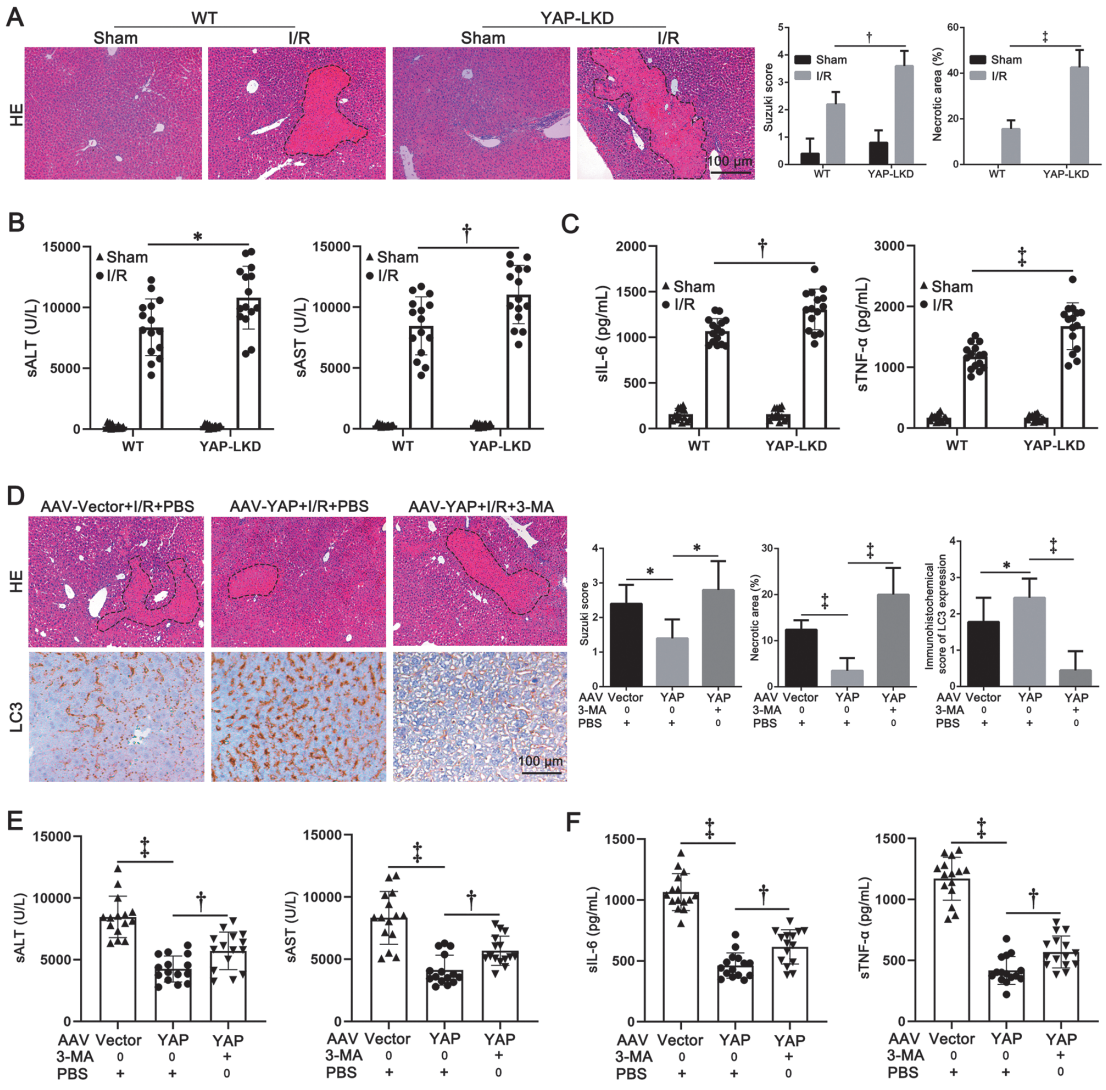

Figure 2: The protective effect of YAP on HIRI depends on activating autophagy. (A–C) Liver samples from WT mice and YAP-LKD mice in the sham group or I/R group were collected. HE staining was analyzed microscopically; Suzuki score and necrosis area were examined; serum levels of ALT, AST, and cytokines (IL-6 and TNF-α) were determined (n = 15). (D–F) WT mice subjected to I/R were then treated with 3-MA following the administration of AAV-vector or AAV-YAP. HE staining and immunohistochemical staining for LC3 were analyzed microscopically; Suzuki score, necrosis area, and the counts of LC3 positive cells were examined; serum levels of ALT, AST, and cytokines (IL-6 and TNF-α) were determined (n = 15). Statistical analyses were performed by Student's t-test, $^{*}P$ <0.05, $^{\dagger}P$ <0.01, $^{\ddagger}P$ <0.001 compared between groups. 3-MA: 3-methyladenine; AAV: Adeno-associated virus; HE: Hematoxylin-eosin; HIRI: Hepatic ischemia-reperfusion injury; I/R: Ischemia/reperfusion; LC3: Light chain 3; LKD: Liver-specific knockdown; PBS: phosphate buffer saline; sAST: Serum aspartate transaminase; sALT: Serum alanine transaminase; sIL-6: Serum interleukin 6; sTNF-α: Serum tumor necrosis factor-α; WT: Wild-type; YAP: Yes-associated protein.

administration of 3-MA to inhibit autophagy in AAV-YAP mice, there was a marked increase in liver Suzuki score, necrotic area, and elevated liver enzymes, as well as significantly upregulated inflammatory cytokines [P <0.05, Figure 2D-F]. This suggests that the previously observed protective effect of YAP overexpression in I/R was abolished when autophagy was inhibited.

YAP-mediated autophagy protected against HIRI by inhibiting apoptosis via reducing ROS and stabilizing mitochondria

Apoptosis is the primary manifestation of HIRI and is closely related to autophagy. Then we explored whether YAP-mediated autophagy protected against HIRI by modulating apoptosis. As shown in Supplementary Figure 3A [http://links.lww.com/CM9/B588], the pro-apoptotic proteins Bax and cleaved-caspase3 were upregulated and the anti-apoptotic protein BCL-2 was downregulated in YAP-LKD mice compared to WT mice under HIRI. Tunel staining results also showed that the apoptotic hepatocytes from *YAP* knockdown mice were markedly increased compared with that from WT counterparts [Figure 3A]. And the overexpressed YAP decreased hepatocyte apoptosis. While WT mice were treated with the autophagy inhibitor after AAV-YAP transfection, cell apoptosis was upregulated, as demonstrated by the western blotting analysis and Tunel staining results [Figure 3B; Supplementary Figure 3B, http://links.lww.com/CM9/B588]. The above results revealed that YAP alleviates HIRI by mediating autophagy to inhibit apoptosis.

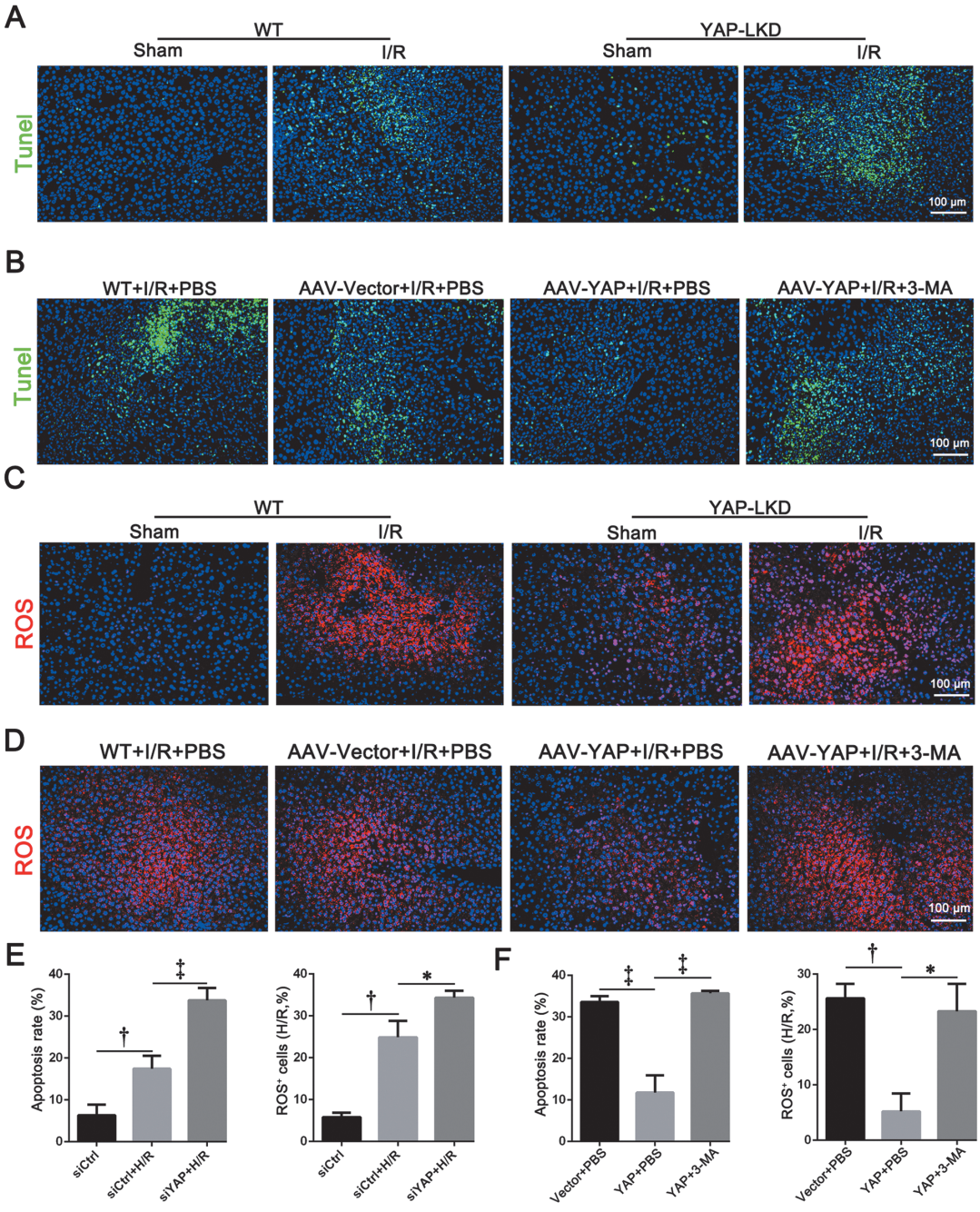

Figure 3: YAP-mediated autophagy inhibits apoptosis of hepatocytes during HIRI. (A) Representative fluorescent Tunel staining of liver sections from WT mice and YAP-LKD mice in the sham group or I/R group. (B) WT mice subjected to I/R were then treated with 3-MA following the administration of AAV-vector or AAV-YAP. The apoptotic activity was analyzed by fluorescent Tunel staining. (C) Representative fluorescent ROS staining of liver sections from WT mice and YAP-LKD mice in the sham group or I/R group. (D) WT mice subjected to I/R were then treated with 3-MA following the administration of AAV-vector or AAV-YAP. ROS accumulation was analyzed by fluorescent ROS staining. Scale bar, 100 μm. The mitochondrial ROS levels, and apoptotic rates were examined by FACS via labelling with MitoSOX and annexin-V/FITC. All statistical analyses were performed by Student's *t*-test, $^{*}P$ <0.05, $^{\dagger}P$ <0.01, $^{\ddagger}P$ <0.001 compared between groups. 3-MA: 3-methyladenine; AAV: Adeno-associated virus; FACS: Fluorescence activating cell sorter; LKD: Liver-specific knockdown; HIRI: Hepatic ischemia-reperfusion injury; I/R: Ischemia/reperfusion; Tunel: Terminal deoxynucleotidyl transferase-mediated dUTP-digoxigenin nick end labeling; PBS: Phosphate buffer saline; ROS: Reactive oxygen species; WT: Wild-type; YAP: Yes-associated protein.

Oxidative stress induced by reperfusion is considered to mediate and aggravate I/R injury. Given the close relationship between autophagy and oxidative stress, we further explored whether YAP dependent autophagy protected against apoptosis by reducing ROS. As the immunofluorescence results shown in Figure 3C, ROS levels were upregulated in YAP-LKD mice compared to WT mice. And overexpressed YAP decreased ROS levels in WT mice. Furthermore, administration of 3-MA after AAV-YAP transfection upregulated the accumulation of ROS [Figure 3D]. We then further traced the ROS (using MitoSox) and apoptosis (using Annexin-V/FITC) activity through flow cytometry using the H/R cell model *in vitro*. Consistent with the *in vivo* results mentioned

above, knockdown of *YAP* significantly increased mitochondrial ROS and cell apoptotic levels during H/R stress compared to control group [P <0.05; Figure 3E; Supplementary Figure 3C, D, http://links.lww.com/CM9/B588]. Furthermore, overexpressed YAP remarkedly decreased mitochondrial ROS levels and cell apoptotic rates, and the protective effect of YAP was further diminished by inhibiting autophagy with 3-MA [P <0.05; Figure 3F; Supplementary Figure 3E, F, http://links.lww.com/CM9/B588]. Taken together, these results indicated that YAP protected against HIRI by inhibiting apoptosis via reducing ROS and stabilizing mitochondria through activating autophagy.

YAP-mediated autophagy depended on JNK activation during HIRI

After confirming that YAP attenuates I/R injury by activating autophagy via inhibiting apoptosis, we further explored its underlying mechanisms. Akt, Erk, p38, and JNK pathways were reported to be involved in cell survival during stress environment.[22] As shown in Figure 4A, Akt, p38, Erk, and JNK were vigorously phosphorylated during I/R injury, while only JNK phosphorylation was restrained after liver-specific *YAP* knockdown. The IHC results further confirmed that enhanced JNK phosphorylation during I/R was suppressed after *YAP* knockdown [Figure 4B]. Additionally, YAP exerted its function mainly by promoting the transcription of target genes through interaction with the transcription factors of the transcriptional enhanced associate domain (TEAD) family. We first confirmed the nuclear enrichment of YAP during I/R via western blotting analysis [Figure 4C], suggesting the possibility that YAP exerted its function by entering the nucleus and binding to TEAD. Moreover, YAP5SA and YAP5SAS94A plasmids were constructed as the previous study described,[23] which promoted the transcriptional activation of YAP and interrupted the physical interaction of YAP with TEADs, respectively. Immunoprecipitation revealed that the introduction of a mutation at the TEAD-binding site (S94A) inhibited the JNK interaction with YAP [Figure 4D]. Furthermore, when THLE2 cells subjected to H/R stress were treated with the YAP-TEAD interaction inhibitor VP after YAP plasmid transfection, it was observed that JNK phosphorylation was fully restrained, autophagy-related proteins including LC3B and Atg5 expression were markedly reduced [Figure 4E]. These results suggested that I/R-induced YAP nuclear translocation might activate JNK through binding to the transcription factor TEAD.

We then detected whether YAP induced autophagy by activating JNK. Subsequently, normal hepatocyte THLE2 cells subjected to H/R were treated with the JNK inhibitor SP600125 after YAP plasmid transfection. The results of western blotting analysis revealed that LC3B and Atg5 expression were decreased after being treated with SP600125 [Figure 4F]. As the fluorescence results also shown, the increased autophagy levels and autophagy flux induced by YAP overexpression were restrained after JNK inhibition [P <0.05, Figure 4G]. Furthermore, to confirm that YAP-mediated autophagy during I/R is JNK-dependent in the *in vivo* models, WT mice were treated with the SP600125 after AAV-YAP transfection. As the western blotting analysis results shown in Figure 4H, similar results to the *in vitro* experiments were observed in the mouse warm I/R model, which showed that the enhanced expression of autophagy-related protein by AAV-YAP transfection was decreased after SP600125 treatment. Therefore, these results indicated that YAP-mediated autophagy induction during hepatic I/R depended on the activation of JNK.

Protective effect of YAP-mediated autophagy against hepatic I/R depended on JNK activation

After confirming that YAP-mediated autophagy depended on JNK activation, we further verified the protective effect of JNK on hepatocytes oxidative stress and apoptosis during HIRI. Subsequently, THLE2 cells subjected to H/R stress were treated with JNK inhibitor SP600125 after YAP plasmid transfection. As the flow cytometry results shown in Supplementary Figure 4A and B[http://links.lww.com/CM9/B588], the decreased mitochondrial ROS level observed in YAP overexpressed cells was upregulated after SP600125 treatment. In addition, the inhibition of JNK promoted cell apoptosis. To further confirm that YAP-mediated protection during I/R is JNK-dependent in the *in vivo* model, WT mice subjected to IRI were treated with SP600125 after AAV-YAP transfection. Consistent with the *in vitro* results, accumulation of ROS and apoptotic activity were remarkably increased in YAP overexpressed mice after SP600125 treatment [Figure 5A]. In addition, western blotting analysis results also showed that the inhibition of JNK promoted cell apoptosis by the increased protein levels of Bax and cleaved-caspase-3 and decreased BCL-2 levels [Figure 5B].

Then, we further evaluated the role of JNK in the protective effect of YAP-mediated autophagy during HIRI. As the results shown, JNK inhibition reduced autophagy levels and weaken YAP-mediated liver protection against I/R injury as demonstrated by increased Suzuki score and necrosis area, serum ALT/AST levels, and inflammatory cytokines (serum IL-6 and TNF-α) [P <0.05, Figure 5C–E]. Moreover, liver grafts from LT patients were further used to evaluate the relationship between YAP, autophagy (indicated by LC3), and JNK during HIRI. We observed that JNK phosphorylation showed a similar trend to YAP and autophagy levels during the OLT by western blot analysis [Figure 5F]. In addition, the expression level of p-JNK protein was found to be correlated with YAP protein levels, as well as with LC3 [P <0.05, Figure 5G; Supplementary Figure 4D, E, http://links.lww.com/CM9/B588]. Further, the immunofluorescence staining results revealed that most of the LC3-positive cells with enriched nuclear YAP also expressed p-JNK [Supplementary Figure 4C, http://links.lww.com/CM9/B588].

Discussion

I/R remains a common cause of liver dysfunction during and after LT, hepatectomy, and shock. There is no

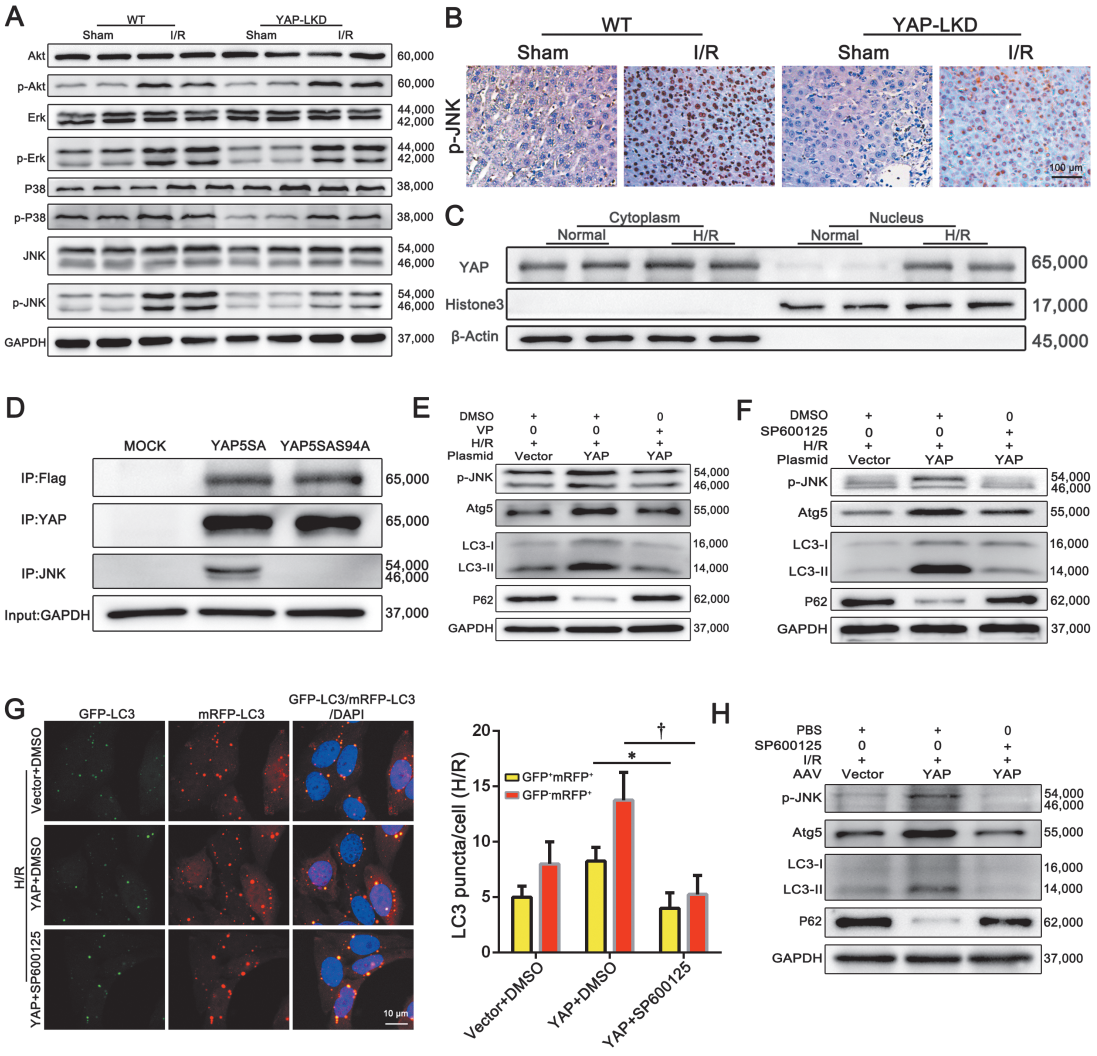

Figure 4: YAP-mediated autophagy depends on JNK activation during HIRI. (A–B) Liver samples from WT mice and YAP-LKD mice in the sham group or I/R group were collected. The protein levels of Akt, Erk, JNK, and p38 were analyzed by western blotting analysis; the expression of p-JNK was determined by immunohistochemical staining; (C) The expression YAP of cytosolic and nuclear-enriched fractions was examined by western blotting analysis. β-actin and Histone 3 were used as loading controls of cytosolic and nuclear fractions, respectively. (D) THLE2 cells were transfected with YAP-5SA and/or YAPS94A plasmids. Cells were then subjected to immunoprecipitation using an anti-YAP antibody and JNK antibody. (E) THLE2 cells subjected to H/R were then treated with VP following the administration of YAP-vector or YAP plasmids. Cells were then harvested for western blotting analysis of p-JNK, Atg5, LC3, and P62. (F) THLE2 cells subjected to H/R were then treated with SP600125 following the administration of YAP-vector or YAP plasmids. Cells were then harvested for western blotting analysis of p-JNK, Atg5, LC3, and P62. (G) THLE2 cells subjected to H/R were transfected with GFP-mRFP-LC3 and then treated with SP600125 following the administration of YAP-vector or YAP plasmids. The autophagy activities were determined by immunofluorescence. (H) WT mice subjected to I/R were then treated with SP600125 following the administration of AAV-vector or AAV-YAP. The protein levels of p-JNK, Atg5, LC3, and P62 were determined by western blotting analysis. All statistical analyses were performed by Student's *t*-test, $^{*}P<0.05$ and $^{\dagger}P<0.01$ compared between groups. ALT: Alanine transaminase; Akt: Phospho Thr308; Atg5: Autophagy-related gene 5; DMSO: Dimethyl sulfoxide; Erk: Extracellular regulated protein kinases; GFP: Green fluorescent protein; HIRI: Hepatic ischemia-reperfusion injury; H/R: Hypoxia/reoxygenation; I/R: Ischemia/reperfusion; JNK: rhAP1 (c-Jun) N-terminal kinase; LC3: Light chain 3; LKD: Liver-specific knockdown; mRFP: Monomeric red fluorescent protein; p62: Sequestosome-1; p-Akt: Phospho-Akt; p-Erk: Phospho-Erk; p-JNK: Phospho-JNK; p-p38: Phospho-p38; p-YAP: Phospho-YAP;VP: Verteporfin; WT: Wild type; YAP: Yes-associated protein.

approved pharmacologic treatment for I/R and its underlying mechanisms remain inconclusive. In the study, we found that YAP was nuclear enriched and positively correlated with the autophagic level of hepatocytes in the post-reperfusion human liver grafts. I/R models with liver-specific *YAP* knockdown mice and cell line were established, and we observed that YAP deficiency inhibited autophagy both in the *in vitro* and *in vivo* models. These results were also confirmed in the OLT patient samples. Specifically, YAP protected against HIRI by inhibiting apoptosis via reducing ROS, which was mediated by activating autophagy. Moreover, the regulation of autophagy by YAP was mediated by JNK signaling through binding to TEAD.

As the key effector of the Hippo pathway, YAP has been reported to be involved in various physiological and pathological processes.[23] In the present study, YAP was found to be significantly upregulated and nuclear enriched in liver grafts after perfusion, suggesting its importance during HIRI. Autophagy is an evolutionarily

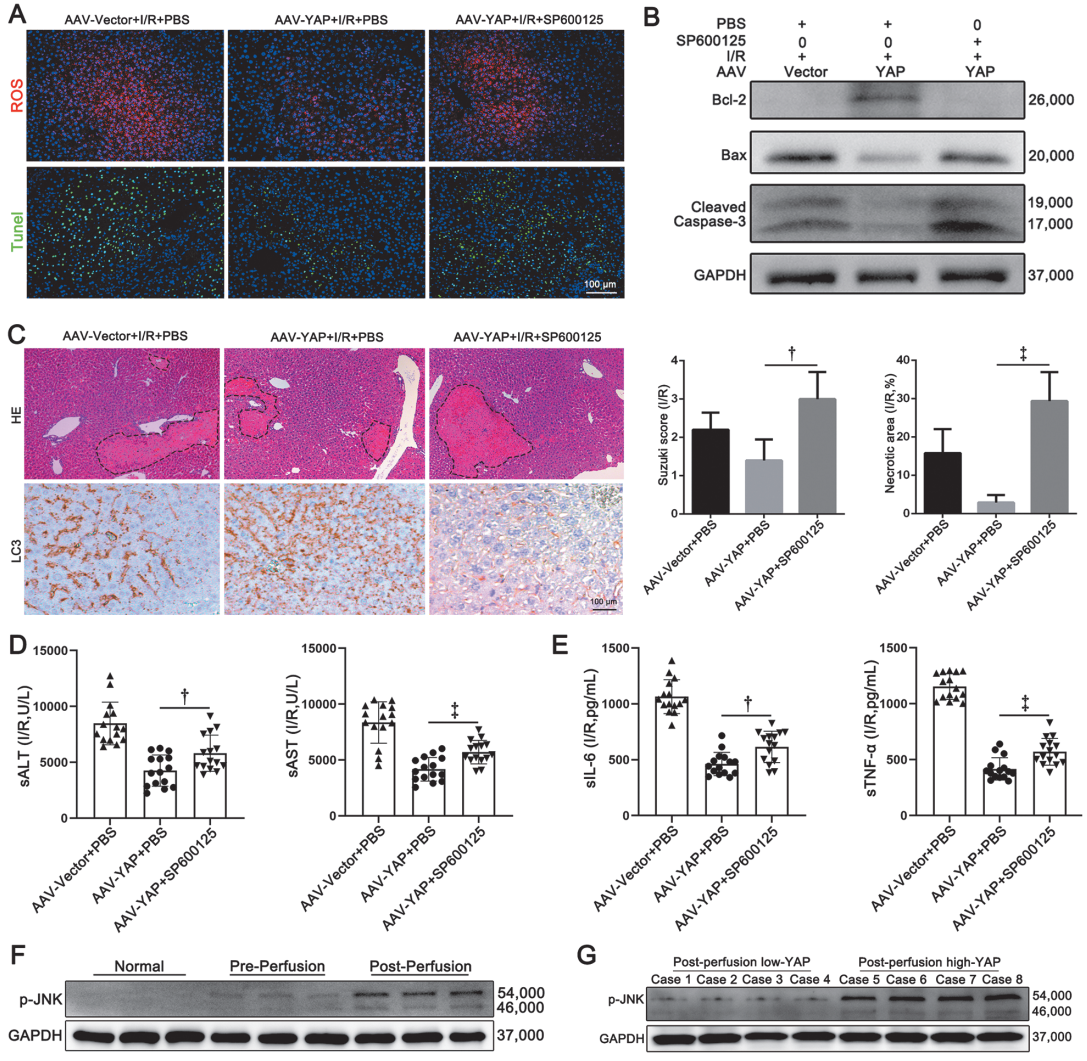

Figure 5: YAP-mediated autophagy depends on JNK activation during HIRI. (A–B) WT mice subjected to I/R were then treated with SP600125 following the administration of AAV-vector or AAV-YAP. The ROS levels were examined by ROS staining and the apoptotic rates were analyzed by Tunel staining (A); the expression of BCL-2, Bax, and Cleaved-caspase3 were determined by western blotting analysis(B). (C–E) WT mice subjected to I/R were then treated with SP600125 following the administration of AAV-vector or AAV-YAP. Liver sections were stained with HE and LC3 (n = 15) (C) Serum levels of ALT, AST (D), and cytokines (IL-6 and TNF-α) (E) were analyzed. (F) Protein levels of p-JNK in normal, peri- and post-reperfusion liver samples from patients were determined by western blotting analysis. (G) Representative immunoblotting profiles of YAP and p-JNK in liver samples were shown. All statistical analyses were performed by Student's t-test, $^{*}P$ <0.05, $^{\dagger}P$ <0.01, $^{\ddagger}P$ <0.001 compared between groups. AAV: Adeno-associated virus; Bax: BCL2-associated X; BCL-2: B-cell lymphoma-2; H/R: Hypoxia-reoxygenation; I/R: Ischemia/reperfusion; LC3: Light chain 3; PBS: phosphate buffer saline; p-JNK: rhAP1 Phospho- (c-Jun) N-terminal kinase; ROS: Reactive oxygen species; sALT: Serum alanine transaminase; sAST: Serum aspartate transaminase; sIL-6: Serum interleukin 6; sTNF-α: Serum tumor necrosis factor-α; Tunel: Terminal deoxynucleotidyl transferase-mediated dUTP-digoxigenin nick end labeling; WT: Wild-type; YAP: Yes associated protein.

conserved damaged protein degradation system that is involved in the regulation of homeostasis under various cellular stress conditions, including nutrient deficiency, ischemia/hypoxia, and inflammation. The relationship between YAP and autophagy has been previously explored by some researchers but remains elusive. Liang *et al*[24] demonstrated that impaired autophagy promoted the accumulation of YAP in tuberous sclerosis complex (TSC) 1/2 deficient cells in an mTOR-dependent manner. While Pavel *et al*[25] reported that YAP and transcriptional coactivator with PDZ-binding motif (TAZ) promoted autophagy through transcriptional regulation of myosin-II. In this study, we investigated the relationship of YAP and autophagy during HIRI given the fact that HIRI served as a common complication of hepatic surgeries. We found that YAP expression was increased in the post-reperfusion liver tissues from LT patients and was significantly correlated with autophagy marker protein LC3 expression, indicating a strong association between the two. Then, we constructed both *in vitro* and *in vivo* models of hypoxia and reoxygenation which simulated I/R to determine whether YAP affected the activation of autophagy. Similar to the patient samples, we found that YAP expression significantly affected the level of autophagy, which provided the evidence for the regulation of YAP on autophagy. What's more, we explored the regulation mechanism in the *in vivo* HIRI model. In order to avoid the disturbance caused by

systemic gene knockdown that affected multiple organs and various cellular functions, liver-specific *YAP* knockdown mice were constructed using a *Cre/loxP* recombination enzyme system to establish the HIRI model, in which only the expression level of *YAP* in the liver tissue was precisely knocked down. We found that the activated autophagy of hepatocytes induced by I/R was significantly downregulated after *YAP* knockdown, confirming the regulatory role of YAP on autophagy activation, at least in HIRI.

The role of autophagy in I/R injury remains controversial. Although autophagy is generally considered to be protective in the I/R injury, excessive or defective autophagy is believed to lead to the degradation of important proteins or organelles and promotes cell death, thus aggravating I/R injury.[26] In contrast to the dubious role of autophagy, the protective role of YAP in I/R injury is relatively clear. Several studies have indirectly or directly pointed out the beneficial role of YAP in I/R injury.[17,18] However, up to date, precise models used to accurately regulate the expression of YAP in the liver to explore its role in I/R injury have been lacking, and whether the protective effect of YAP is dependent on activating autophagy has not been reported. In our study, a liver-specific *YAP* knockdown mouse model, a YAP overexpressed hepatocyte cell model, and a *YAP* knockdown cell model were constructed. The results of human patient samples, the *YAP* knockdown mice model, and the cell model all suggested the protective role of YAP in the I/R injury. This protective effect disappears after the use of autophagy inhibitor 3-MA, indicating that inhibition of autophagy weakens the protective effect of YAP on I/R injury, suggesting that autophagy inhibition weakened YAP-mediated protective effect on cell survival, accompanied by significant up-regulation of apoptosis levels. Accordingly, overexpression of YAP accelerates the clearance of mitochondrial ROS and maintains mitochondrial membrane stability, which is reversed by inhibition of autophagy. Apoptosis, which is caused by reperfusion-induced oxidative stress, has been widely recognized as the key mechanism that aggravates I/R injury. Thus, YAP exerts its protective role in HIRI via an autophagy-dependent manner.

JNK is a serine/threonine protein kinase that belongs to the family of mitogen-activated protein kinase (MAPK), which is involved in the regulation of cell proliferation, differentiation, and apoptosis.[27] JNK is activated by the dual phosphorylation of threonine and tyrosine residues by two MAPK kinases. Activated JNK can regulate or directly phosphorylate the expression of various transcription factors such as activating transcription factor (ATF), and c-Jun. Previous studies have shown that JNK is linked to autophagy by regulating the expression of autophagy genes in various ways.[28,29] In this study, we also found that p-JNK was significantly upregulated during autophagy activation during HIRI. Surprisingly, only JNK is down-regulated most significantly after *YAP* knockdown, given the facts that Akt, p-38, and Erk signaling pathways are all considered to be important transducers in promoting cell survival and proliferation.[14] Previous studies have reported that YAP regulates JNK expression in some disease models, such as atherosclerosis, basal cell carcinoma, and *Drosophila* cell invasion.[30–32] In fact, YAP regulated the expression of target genes by binding to the transcription factor TEAD, which is the primary way that YAP functions. In this study, we investigated the novel mechanism in which YAP interacts with TEAD to regulate JNK expression and activate autophagy. Our immunoprecipitation assay showed that overexpression of YAP promoted the phosphorylation of JNK, while mutations at the YAP–TEAD binding site reversed the promoting effect of YAP on JNK activation, which was further confirmed by the application of YAP–TEAD binding disruptor VP *in vitro*. In addition, YAP overexpression in THLE2 cells accelerated hypoxic reoxygenation-induced autophagy levels, which were reversed by JNK inhibition. These data suggested that JNK was an executor of YAP-mediated autophagy in HIRI and was regulated by the interaction between YAP and TEAD. However, the detailed signaling pathway of YAP–TEAD regulated JNK activation is still unclear. Whether YAP directly affects the expression and activation of JNK through binding to TEAD or indirectly promotes the activation of JNK by promoting the expression of other genes targeting JNK remains to be further studied.

In conclusion, our experiments demonstrated that the protective effect of YAP in hepatic I/R was strongly dependent on the activation of autophagy, which reduced apoptosis by reducing mitochondrial ROS production and maintaining mitochondrial membrane stability. In addition, JNK signaling is the major executor of YAP-mediated autophagy and is regulated by YAP–TEAD binding. Therefore, we propose that Hippo (YAP)–JNK–autophagy axis plays an important role in regulating HIRI, and targeting this signaling axis may provide a new strategy for the prevention and treatment of IR injury.

Funding

This study was supported by grants from the National Natural Science Foundation of China (Nos. 82100691, 82070673, and 81870447), the Guangdong Natural Science Foundation (No. 2021A1515010726), the China Postdoctoral Science Foundation (No. 2021M693631), and the Medical Scientific Research Foundation of Guangdong Province of China (No. A2021160).

Conflicts of interest

None.

References

1. Fuertes-Agudo M, Luque-Tévar M, Cucarella C, Brea R, Boscá L, Quintana-Cabrera R, *et al*. COX-2 expression in hepatocytes improves mitochondrial function after hepatic ischemia-reperfusion injury. Antioxidants (Basel) 2022;11:1724. doi: 10.3390/antiox11091724.
2. Obert DP, Wolpert AK, Korff S. Modulation of endoplasmic reticulum stress influences ischemia-reperfusion injury after hemorrhagic shock. Shock 2019;52:76–84. doi: 10.1097/SHK.0000000000001298.
3. Zhou J, Hu M, He M, Wang X, Sun D, Huang Y, *et al*. TNFAIP3 interacting protein 3 is an activator of Hippo-YAP signaling

protecting against hepatic ischemia/reperfusion injury. Hepatology 2021;74:2133–2153. doi: 10.1002/hep.32015.
4. Ito T, Naini BV, Markovic D, Aziz A, Younan S, Lu M, *et al*. Ischemia-reperfusion injury and its relationship with early allograft dysfunction in liver transplant patients. Am J Transplant 2021;21:614–625. doi: 10.1111/ajt.16219.
5. Durgan J, Florey O. Many roads lead to CASM: Diverse stimuli of noncanonical autophagy share a unifying molecular mechanism. Sci Adv 2022;8:eabo1274. doi: 10.1126/sciadv.abo1274.
6. Gracia-Sancho J, Guixe-Muntet S. The many-faced role of autophagy in liver diseases. J Hepatol 2018;68:593–594. doi: 10.1016/j.jhep.2017.09.015.
7. Pena-Martinez C, Rickman AD, Heckmann BL. Beyond autophagy: LC3-associated phagocytosis and endocytosis. Sci Adv 2022;8:eabn1702. doi: 10.1126/sciadv.abn1702.
8. Ashrafizadeh M, Ahmadi Z, Farkhondeh T, Samarghandian S. Autophagy as a molecular target of quercetin underlying its protective effects in human diseases. Arch Physiol Biochem 2022; 128:200–208. doi: 10.1080/13813455.2019.1671458.
9. Liao X, Sluimer JC, Wang Y, Subramanian M, Brown K, Pattison JS, *et al*. Macrophage autophagy plays a protective role in advanced atherosclerosis. Cell Metab 2012;15:545–553. doi: 10.1016/j.cmet.2012.01.022.
10. Kaushal GP, Chandrashekar K, Juncos LA. Molecular interactions between reactive oxygen species and autophagy in kidney disease. Int J Mol Sci 2019;20:3791. doi: 10.3390/ijms20153791.
11. Popov SV, Mukhomedzyanov AV, Voronkov NS, Derkachev IA, Boshchenko AA, Fu F, *et al*. Regulation of autophagy of the heart in ischemia and reperfusion. Apoptosis 2023;28:55–80. doi: 10.1007/s10495-022-01786-1.
12. Chen J, You H, Li Y, Xu Y, He Q, Harris RC. EGF receptor-dependent YAP activation is important for renal recovery from AKI. J Am Soc Nephrol 2018;29:2372–2385. doi: 10.1681/ASN.2017121272.
13. Wei N, Pu Y, Yang Z, Pan Y, Liu L. Therapeutic effects of melatonin on cerebral ischemia reperfusion injury: Role of YAP-OPA1 signaling pathway and mitochondrial fusion. Biomed Pharmacother 2019;110:203–212. doi: 10.1016/j.biopha.2018.11.060.
14. Matsuda T, Zhai P, Sciarretta S, Zhang Y, Jeong JI, Ikeda S, *et al*. NF2 activates Hippo signaling and promotes ischemia/reperfusion injury in the heart. Circ Res 2016;119:596–606. doi: 10.1161/CIRCRESAHA.116.308586.
15. Castellan M, Guarnieri A, Fujimura A, Zanconato F, Battilana G, Panciera T, *et al*. Single-cell analyses reveal YAP/TAZ as regulators of stemness and cell plasticity in glioblastoma. Nat Cancer 2021;2:174–188. doi: 10.1038/s43018-020-00150-z.
16. Yu FX, Zhao B, Guan KL. Hippo pathway in organ size control, tissue homeostasis, and cancer. Cell 2015;163:811–828. doi: 10.1016/j.cell.2015.10.044.
17. Zhou LY, Zhai M, Huang Y, Xu S, An T, Wang YH, *et al*. The circular RNA ACR attenuates myocardial ischemia/reperfusion injury by suppressing autophagy via modulation of the Pink1/FAM65B pathway. Cell Death Differ 2019;26:1299–1315. doi: 10.1038/s41418-018-0206-4.
18. Liu CY, Zhang YH, Li RB, Zhou LY, An T, Zhang RC, *et al*. LncRNA CAIF inhibits autophagy and attenuates myocardial infarction by blocking p53-mediated myocardin transcription. Nat Commun 2018;9:29. doi: 10.1038/s41467-017-02280-y.
19. Chen X, Zhang J, Xia L, Wang L, Li H, Liu H, *et al*. Beta-arrestin-2 attenuates hepatic ischemia-reperfusion injury by activating PI3K/Akt signaling. Aging (Albany NY) 2020;13:2251–2263. doi: 10.18632/aging.202246.
20. Brunt VE, Wiedenfeld-Needham K, Comrada LN, Minson CT. Passive heat therapy protects against endothelial cell hypoxia-reoxygenation via effects of elevations in temperature and circulating factors. J Physiol 2018;596:4831–4845. doi: 10.1113/JP276559.
21. Suzuki S, Toledo-Pereyra LH, Rodriguez FJ, Cejalvo D. Neutrophil infiltration as an important factor in liver ischemia and reperfusion injury. Modulating effects of FK506 and cyclosporine. Transplantation 1993;55:1265–1272. doi: 10.1097/00007890-199306000-00011.
22. Goga M, Kello M, Vilkova M, Petrova K, Backor M, Adlassnig W, *et al*. Oxidative stress mediated by gyrophoric acid from the lichen *Umbilicaria hirsuta* affected apoptosis and stress/survival pathways in HeLa cells. BMC Complement Altern Med 2019;19: 221. doi: 10.1186/s12906-019-2631-4.
23. Kim MH, Kim CG, Kim SK, Shin SJ, Choe EA, Park SH, *et al*. YAP-induced PD-L1 expression drives immune evasion in BRAFi-resistant melanoma. Cancer Immunol Res 2018;6:255–266. doi: 10.1158/2326-6066.CIR-17-0320.
24. Liang N, Zhang C, Dill P, Panasyuk G, Pion D, Koka V, *et al*. Regulation of YAP by mTOR and autophagy reveals a therapeutic target of tuberous sclerosis complex. J Exp Med 2014;211: 2249–2263. doi: 10.1084/jem.20140341.
25. Pavel M, Renna M, Park SJ, Menzies FM, Ricketts T, Füllgrabe J, *et al*. Contact inhibition controls cell survival and proliferation via YAP/TAZ-autophagy axis. Nat Commun 2018;9:2961. doi: 10.1038/s41467-018-05388-x.
26. Boz Z, Hu M, Yu Y, Huang XF. N-acetylcysteine prevents olanzapine-induced oxidative stress in mHypoA-59 hypothalamic neurons. Sci Rep 2020;10:19185. doi: 10.1038/s41598-020-75356-3.
27. Lin X, Ye R, Li Z, Zhang B, Huang Y, Du J, *et al*. KIAA1429 promotes tumorigenesis and gefitinib resistance in lung adenocarcinoma by activating the JNK/ MAPK pathway in an m(6)A-dependent manner. Drug Resist Updat 2023;66:100908. doi: 10.1016/j.drup.2022.100908.
28. King KE, Losier TT, Russell RC. Regulation of autophagy enzymes by nutrient signaling. Trends Biochem Sci 2021;46:687–700. doi: 10.1016/j.tibs.2021.01.006.
29. Lin T, Ruan S, Huang D, Meng X, Li W, Wang B, *et al*. MeHg-induced autophagy via JNK/Vps34 complex pathway promotes autophagosome accumulation and neuronal cell death. Cell Death Dis 2019;10:399. doi: 10.1038/s41419-019-1632-z.
30. Maglic D, Schlegelmilch K, Dost AF, Panero R, Dill MT, Calogero RA, *et al*. YAP-TEAD signaling promotes basal cell carcinoma development via a c-JUN/AP1 axis. EMBO J 2018;37:e98642. doi: 10.15252/embj.201798642.
31. Wang L, Luo JY, Li B, Tian XY, Chen LJ, Huang Y, *et al*. Integrin-YAP/TAZ-JNK cascade mediates atheroprotective effect of unidirectional shear flow. Nature 2016;540:579–582. doi: 10.1038/nature20602.
32. Ma X, Wang H, Ji J, Xu W, Sun Y, Li W, *et al*. Hippo signaling promotes JNK-dependent cell migration. Proc Natl Acad Sci U S A 2017;114:1934–1939. doi: 10.1073/pnas.1621359114.

How to cite this article: Zhu SG, Wang XW, Chen HQ, Zhu WF, Li XJ, Cui RW, Yi XM, Chen XL, Li H, Wang GS. Hippo (YAP) – autophagy axis protects against hepatic ischemia-reperfusion injury through JNK signaling. Chin Med J 2024;137:657–668. doi: 10.1097/CM9.0000000000002727